International Journal of Greenhouse Gas Control

Supporting Information for **A tool for first order estimates and optimisation of dynamic storage resource capacity in saline aquifers.**

Silvia De Simone*[a b] and Samuel Krevor[a]

[a] Imperial College London, Dept. of Earth Science and Engineering, London SW7 2AZ, UK
[b] Univ Rennes, CNRS, Géosciences Rennes - UMR 6118, Rennes, France

Contents

*Corresponding author: Silvia De Simone, silviadesi@gmail.com

S1 Pressure response to CO_2 injection into multiple sites

Following Nordbotten et al. (2005), the estimate of the pressure response to CO_2 injection into a single well in a homogeneous reservoir with open boundaries can be simplified into

$$\Delta p(r,t) = \frac{Q\mu_w}{2\pi\kappa H\rho_c} \times \begin{cases} \dfrac{\mu_c}{\mu_w}\ln\left(\dfrac{\psi}{r}\right) + \ln\left(\dfrac{R}{\psi}\right) & , r < \psi \\ \ln\left(\dfrac{R}{r}\right) & , \psi < r < R \\ 0 & , r > R \end{cases} \tag{S1}$$

where $\Delta p(r,t)$ is the pressure variation at time t and distance r from the injection well, Q is the injected mass flow rate, κ is the absolute permeability, H is the reservoir thickness, ρ_c is the CO_2 density, μ_w and μ_c are the brine and CO_2 viscosities, respectively, $R = \sqrt{2.25\kappa t/(\mu_w\alpha)}$ is the pressure propagation radius which expands proportionally with $\sqrt{t}$, α is the total reservoir compressibility, and ψ represents the radius of a fictitious equivalent vertical interface, such that $\psi = \exp(\omega)\xi$, where $\omega = (\mu_c+\mu_w)/(\mu_c-\mu_w)\ln(\sqrt{\mu_c/\mu_w})-1$, $\xi = \sqrt{Qt/(\pi\phi H\rho_c)}$ is the advective propagation distance and ϕ is the porosity.

In the case of closed reservoirs, a simplified solution for pressure can be derived by modifying Eq. (S1) according to the solution for single-phase flow in closed reservoir (Zimmerman, 2018)

$$\Delta p(r,t) = \frac{Q\mu_w}{2\pi\kappa H\rho_c} \times \begin{cases} \dfrac{\mu_c}{\mu_w}\ln\left(\dfrac{\psi}{r}\right) + \ln\left(\dfrac{R_c}{\psi}\right) + \dfrac{2R^2}{2.25R_c^2} - \dfrac{3}{4} & , r < \psi \\ \ln\left(\dfrac{R_c}{r}\right) + \dfrac{2R^2}{2.25R_c^2} - \dfrac{3}{4} & , \psi < r < R_c \\ 0 & , r > R_c \end{cases} \tag{S2}$$

The underlying assumption is that the CO_2 plume radial extension ψ is smaller than the reservoir radius R_c.

In the case of simultaneous injection into multiple sites, the pressure response at location $\mathbf{x}_i$ can be estimated as the superposition of single well pressure responses

$$\Delta p_{sup}(\mathbf{x}_i,t) = \sum_{j=1}^{n} \Delta p(d_{ij},t) \,, \tag{S3}$$

where n is the number of wells, $\Delta p(r,t)$ is the pressure response to a single well injection at distance r from the injection well, while d_{ij} is the distance between the locations $\mathbf{x}_i$ and $\mathbf{x}_j$. Assuming open boundary domain and that the same flow rate is injected at each well, the superposed pressure response at $\mathbf{x}_i$ is estimated as

$$\Delta p_{sup}(\mathbf{x}_i,t) = \frac{Q\mu_w}{2\pi\kappa H\rho_c}\left[\frac{\mu_c}{\mu_w}\ln\left(\frac{\psi}{r_0}\right)+\ln\left(\frac{R}{\psi}\right)+\sum_{j=2}^{n}\ln\left(\frac{R}{d_{ij}}\right)\right] \tag{S4}$$

where r_0 represents the well radius and we have assumed no interference in CO_2 plumes, i.e., $d_{ij}>\psi, \forall j$. A similar expression can be derived for the case of a closed domain. We discuss the applicability of the superposition procedure in Section S3.

S2 Nonlinear $\Delta p/Q$ relationship

The extension of the CO_2 plume is affected by the flow rate, e.g., $\psi \propto \sqrt{Q}$ (see Section S1). This implies that $\Delta p(r,t)$ is not linearly depending on Q for $r<\psi$ (Eqs. (S1) and (S2)), thus the dimensionless overpressure $\Delta p_D(r,t,Q) = \Delta p(r,t)/(Q\mu_w/(2\pi\kappa H\rho_c))$ changes with the flow rate (Figure S1). For both open and closed reservoirs, the difference between the dimensionless overpressure associated with two different flow rates, Q_1 and Q_2, returns, after some algebra

$$\Delta p_D(r,t,Q_2)-\Delta p_D(r,t,Q_1) = -\delta\ln\left(\frac{\psi_2}{\psi_1}\right) = -\frac{\delta}{2}\ln\left(\frac{Q_2}{Q_1}\right)\ , \tag{S5}$$

where $\delta=(\mu_w-\mu_c)/\mu_w$.

However, in the case of closed domains the $\Delta p/Q$ relationship approaches the linearity for large times, as the last two terms on the right hand side of Eq. (S2) dominate (Figure S1 right), such that the difference in Eq. (S5) becomes irrelevant.

In the case of multiple injectors (Eq. (S4)), the difference in dimensionless overpressure in response to two different flow rates, i.e., $\Delta p_{sup_D}(r,t,Q_2)-\Delta p_{sup_D}(r,t,Q_1)$, still returns Eq. (S5), for both open and closed reservoirs. In this case, the nonlinearity of the $\Delta p/Q$ relationship is solely related to the response to the injection into the observation well. This is due to the assumption of non interacting plumes, i.e, $d_{ij}>\psi, \forall j$, which implies that the effect of the injection into the other wells is only associated with the brine viscosity, thus linear. Given the small impact of one injector over multiple, the nonlinearity is weaker than for the single well case and it reduces with increasing well number and for the case of closed reservoirs (Figure S2).

Rearrangement of Eq. (S5) gives

$$\Delta p(r,t,Q_2) = Q_2\left[\frac{\Delta p(r,t,Q_1)}{Q_1} - b\ln\left(\frac{Q_2}{Q_1}\right)\right] \tag{S6}$$

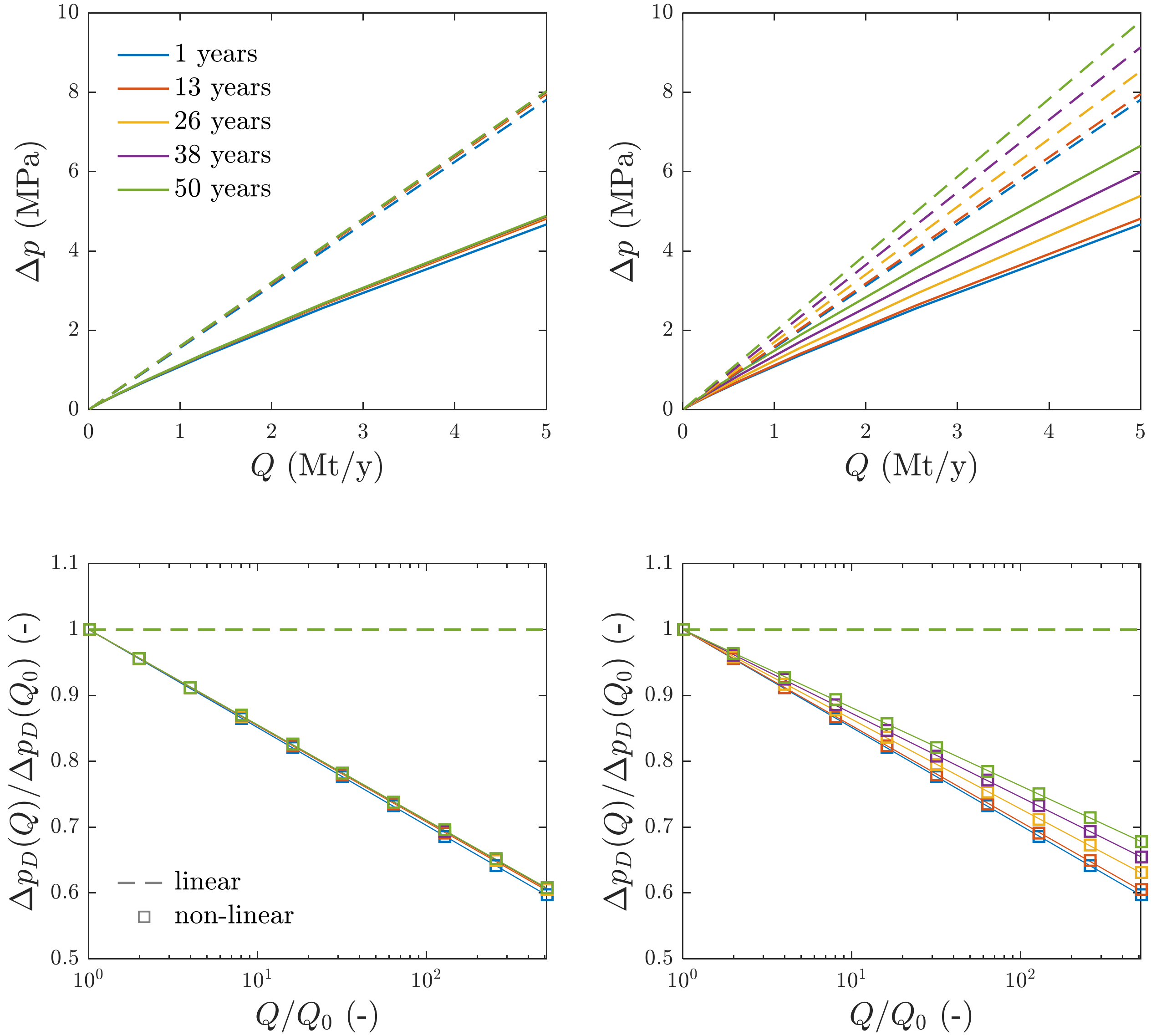

Figure S1: Absolute (top) and dimensionless (bottom) pressure build-up at the injection well under different flow rate scenarios of CO_2 injection. Left and right panels represent the cases of open and closed reservoirs, respectively. Colors correspond to different injection times (from 1 up to 50 years). Solid lines correspond to the solution calculated for each injection rate. Dashed lines represent the pressure build-up calculated from the response to the smallest injection rate, Q_0, by assuming linear $\Delta p/Q$ relationship, while markers represent the extrapolation by means of the nonlinear $\Delta p/Q$ relationship expressed by Eq. (S5).

where $b = (\mu_w - \mu_c)/(4\pi\kappa H \rho_c)$. The inversion of this equation allows for directly estimating the maximum allowable flow rate, after having calculated the overpressure for a reference case (e.g., Q_1) and having imposed the maximum sustainable overpressure (Eq. (5)).

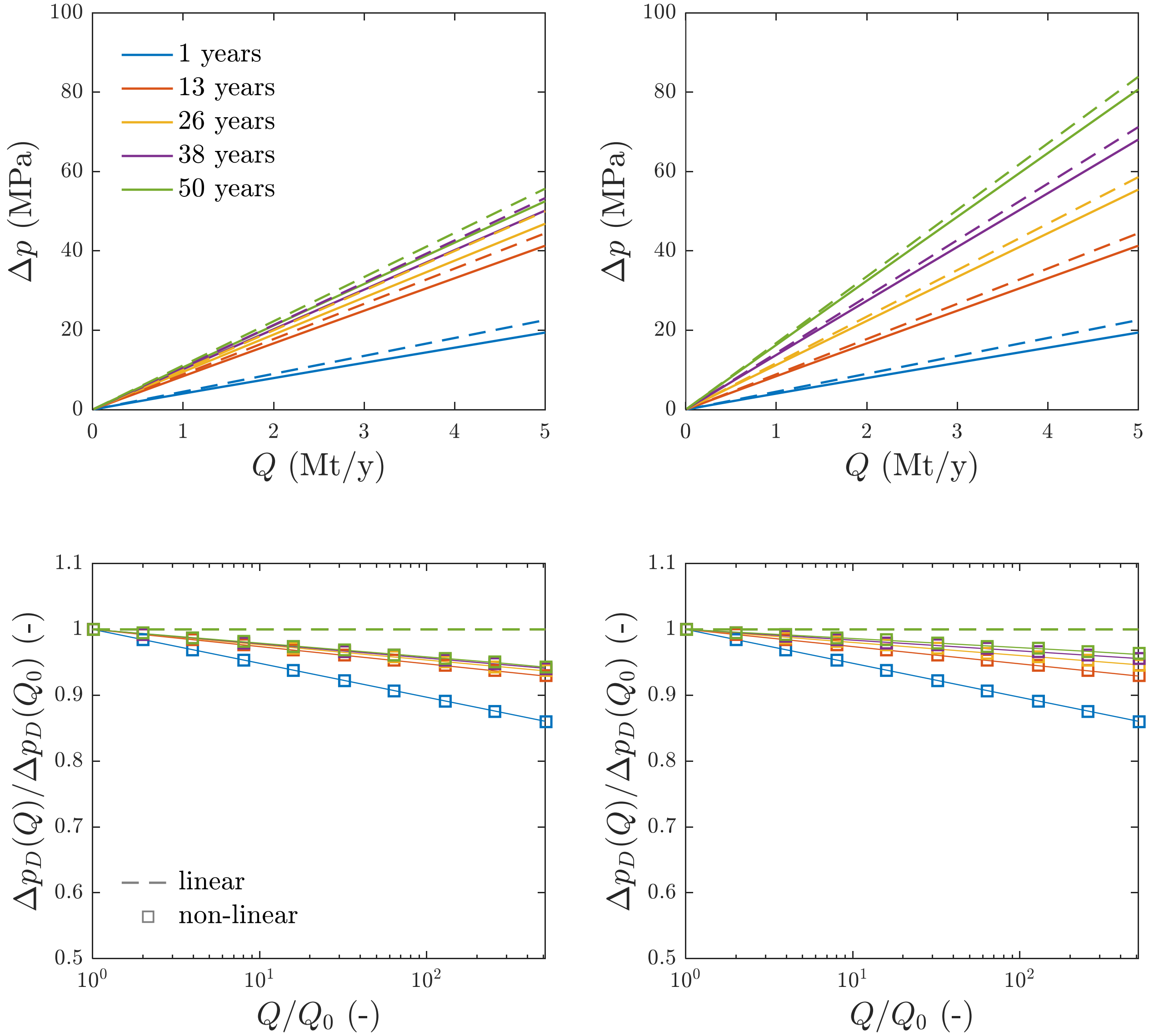

Figure S2: Absolute (top) and dimensionless (bottom) pressure build-up at the central well of a 16 wells scenario under different flow rate of CO_2 injection. Interwell distance is assumed equal to 2 km. Left and right panels represent the cases of open and closed reservoirs, respectively. Colors correspond to different injection times (from 1 up to 50 years). Solid lines correspond to the solution calculated for each injection rate. Dashed lines represent the pressure build-up calculated from the response to the smallest injection rate, Q_0, by assuming linear $\Delta p/Q$ relationship, while markers represent the extrapolation by means of the nonlinear $\Delta p/Q$ relationship expressed by Eq. (S5).

S3 Correction of the superposition error for multiple site scenarios

De Simone et al. (2019) have shown that the application of the superposition principle to the case of multiphase flow incurs an error, which is negligible for small number of wells n. They show that, for multiwell injection into a domain with open boundary condition and $n > 9$, the pressure build-up at the inner-most well is

$$\Delta p_{sup}(\mathbf{x}_i, t) = \frac{Q\mu_w}{2\pi\kappa H\rho_c}\left[\frac{\mu_c}{\mu_w}\ln\left(\frac{\psi}{r_0}\right) + \ln\left(\frac{R}{\psi}\right) + \sum_{j=2}^{n}\ln\left(\frac{R}{d_{ij}}\right) - \frac{n\delta}{4}\ln\left(\frac{R\xi}{d^2}\right)\right] \tag{S7}$$

where the last term represent the error correction, with $\xi = \sqrt{Qt/(\pi\phi H\rho_c)}$, and d is the interwell distance.

Recalling that $\psi \propto \xi$ (see Section S1), the dimensionless overpressure varies with the flow rate such that

$$\Delta p_D(r, t, Q_2) - \Delta p_D(r, t, Q_1) = -\frac{\delta}{2}\left(1 + \frac{n}{4}\right)\ln\left(\frac{Q_2}{Q_1}\right)\ , \tag{S8}$$

which corrects Eq. (S5). Thus, the maximum sustainable flow rate can be still calculated by Eq. (5), but substituting b with $b^* = (\mu_w - \mu_c)(1 + n/4)/(4\pi\kappa H\rho_c)$.

S4 UK site data

The file **UK_data.xlsx** provides the data of the UK sites collected from the CO2Stored database (Energy Technologies Institute LLP, 2018) and used for the calculations.

S5 Storage resources of the UK under different well number limits

Table S1: Maximum storage capacity, V_M, and corresponding scenario of inter-well distance, d, for each of the selected UK sites, for two cases of maximum well number, n. We consider 30 years of continuous injection.

	max $n = 2000$			**max $n = 50$**		
Site name	V_M **(Gt)**	d **(km)**	n	V_M **(Gt)**	d **(km)**	n
Argyll 038 14	1.77	2.1	1600	1.44	11.8	49
Auk 009 28	5.42	1.4	1849	1.94	8.3	49
Auk 020 05'	4.26	1.4	1560	1.14	6.2	49
Auk 022 13	8.38	2.3	1722	1.10	7.5	49
Auk 029 15	15.12	2.5	1764	1.65	8.1	49
Bunter Closure 28	0.20	8.8	2	0.20	8.8	2
Bunter Closure 3'	0.08	5.1	2	0.08	5.1	2
Bunter Closure 35	0.18	7.3	2	0.18	7.3	2
Bunter Closure 36	0.09	4.9	2	0.09	4.9	2
Bunter Closure 37	0.13	5.3	2	0.13	5.3	2
Bunter Closure 39	0.12	4.9	2	0.12	4.9	2
Bunter Sandstone FZ1	2.74	6.0	144	2.62	10.9	42
Collyhurst Sandstone F1	12.90	2.9	484	7.35	7.3	49
Cormorant 003 02	9.26	2.3	240	7.35	4.5	49
Cormorant 009 18	21.00	1.9	484	7.35	2.5	49
Cormorant 211 12	3.10	2.5	72	3.08	3.4	36
Cormorant 211 23	11.24	2.1	506	7.35	5.7	49
Forties 5	4.23	3.2	1369	3.52	16.7	49
Hugin 009 18	0.90	7.0	6	0.90	7.0	6
Mackerel Chalk 022 15	3.68	1.2	1892	1.63	7.5	49
Maureen 2	25.17	4.7	1600	7.35	15.2	49
Mey 5	27.22	5.1	930	7.35	9.4	49
Pentland 009 28	1.92	4.5	36	1.92	4.5	36
Pentland 016 21b	0.90	6.2	12	0.90	6.2	12
Tor Chalk 022 09	4.52	1.4	1849	1.36	7.0	49

S6 Analysis of investment cost and revenues for the Forties 5 and the Bunter Closure 28 sites

Investment cost, I, includes the cost of capture, C_c, transportation, C_t, and storage, C_s. Transportation cost ranges between 1-8 €tCO_2^{-1} for a pipeline of 250 km, depending on the terrain conditions and whether the pipeline is onshore or offshore (IPCC, 2005). We assume a total value of 10 €tCO_2^{-1} for both sites. Storage cost is the sum of different components (drilling costs C_{dr}, fixed costs C_{fx}, surface facilities costs C_{fc}, site development costs C_{sd}, monitoring equipment costs C_{me}), plus an additional operating, maintenance, and monitoring cost C_{ac}. Assumed specific costs are summarized in Table S2. The equations to evaluate the cost of each component and the total cost are the following

$$I = C_c + C_t + C_s \tag{S9}$$

$$C_c = c_c\, M \tag{S10}$$

$$C_t = c_t\, M \tag{S11}$$

$$C_s = \left[n\left(c_{dr}\,\zeta_m + c_{fx} + c_{fc}\right) + C_{sd} + C_{me}\right](1 + C_{ac}) \tag{S12}$$

where M is the mass of CO_2 to store (ton), n is the well number and ζ_m is the average aquifer depth. Note that we have omitted the obvious conversions from k€ to €, necessary to make all costs consistent.

Table S2: Investment costs assumed in the economic model for the case of deep offshore saline formations. The symbol k€ means 1000€, €/t refers to cost per ton of CO_2, €/m refers to cost per meter length of well, €/n refers to cost per well. Data are derived from Carneiro et al. (2015); Mathias et al. (2015); IPCC (2005).

Symbol	**Parameter**	**Value**	**Units**
c_c	Capture cost	50	€/t
c_t	Transportation cost	10	€/t
	Storage Cost		
c_{dr}	drilling	26	k€/m
c_{fx}	fixed cost	8200	k€/n
c_{fc}	surface facilities	6120	k€/n
C_{sd}	site development	24097	k€
C_{me}	monitoring equipment	1530	k€
C_{ac}	additional costs	5	%

For the revenue, we consider five scenarios of revenue between 5 and 200 €tCO_2^{-1}.

Forties 5 and Bunter Closure 28 present very different characteristics and constitute illustrative examples of different kinds of aquifers. The first is a very large reservoir with open hydraulic boundaries. The second is a small stratighraphic trap with closed hydraulic boundaries. Their storage capacity is thus maximized in very different ways.

In the case of Forties 5, the maximum storage capacity increases with the well number until reaching a plateau, where the storage capacity oscillates around a constant value (Fig. S3A and B). For the Bunter Closure 28, the maximum storage capacity is achieved with two wells at very large distance (Fig. S4A and B).

Both capture and transportation cost on one side, and revenue on the other, change linearly with the storage capacity, whereas the storage cost increases linearly with the well number (Fig. S3C and D and Fig. S4C and D). Thus, the net revenue (revenues minus investment) varies with the well number approximately as the storage capacity (see Fig. 11). For large number of wells, however, the storage cost has a stronger impacts on the total cost, with the effect that the maximum revenue corresponds to an intermediate number of wells. Note that storage equals zero for large well numbers, reflecting impossible scenarios.

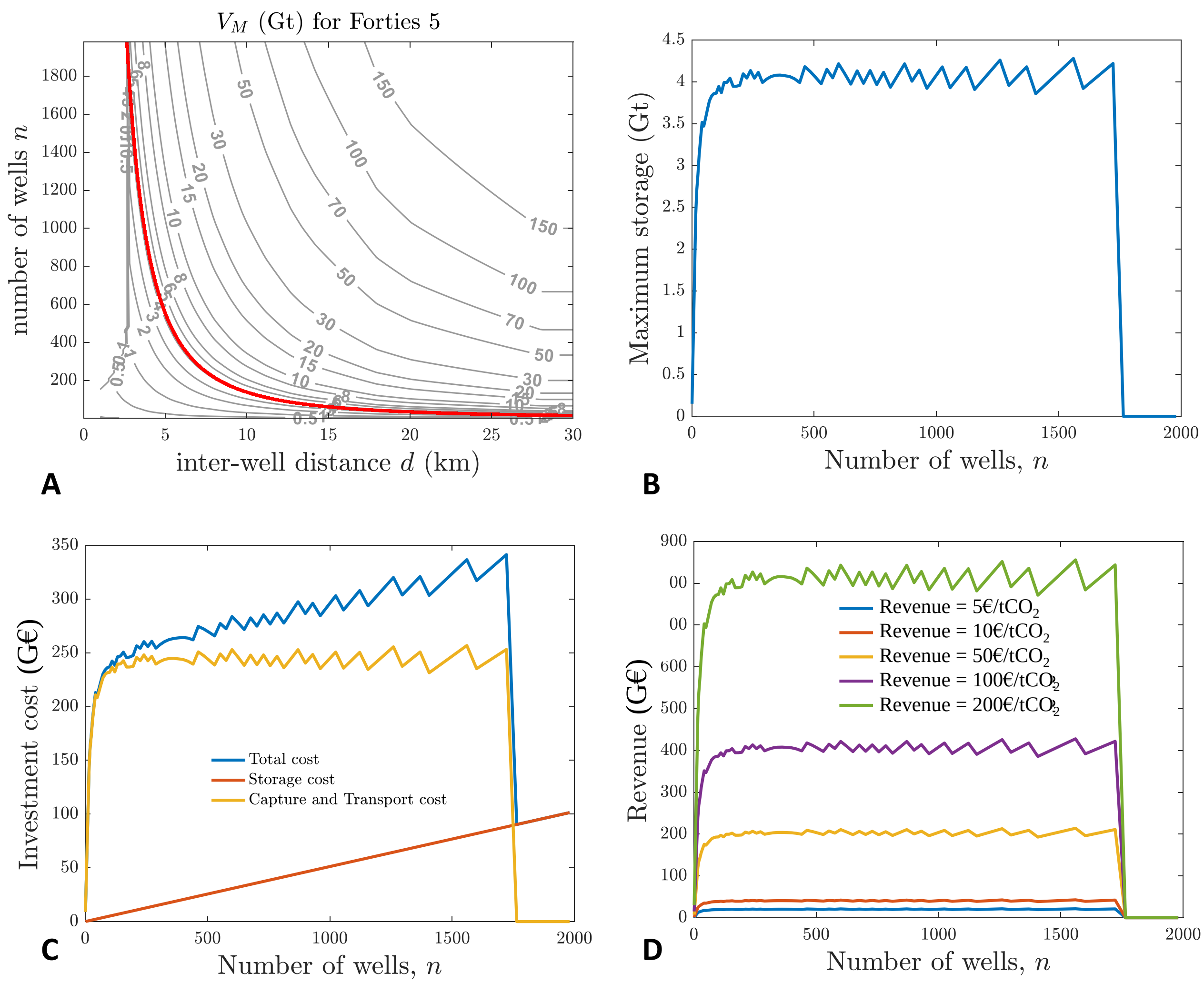

Figure S3: Cost and revenues of 30 years of CO_2 storage at the Forties 5 site under different scenarios of well number and revenue values. A) Pressure-limited scenarios of sustainable injection mass for different well number and distance; plausible scenarios are on the left of the red line. B) Maximum plausible storage capacity for each scenario of well number (corresponding to the region close to the red line in panel A). C) Investment cost for each scenario of well number represented in panel B. D) Revenues for each scenario of well number represented in panel B and for different values of incentive.

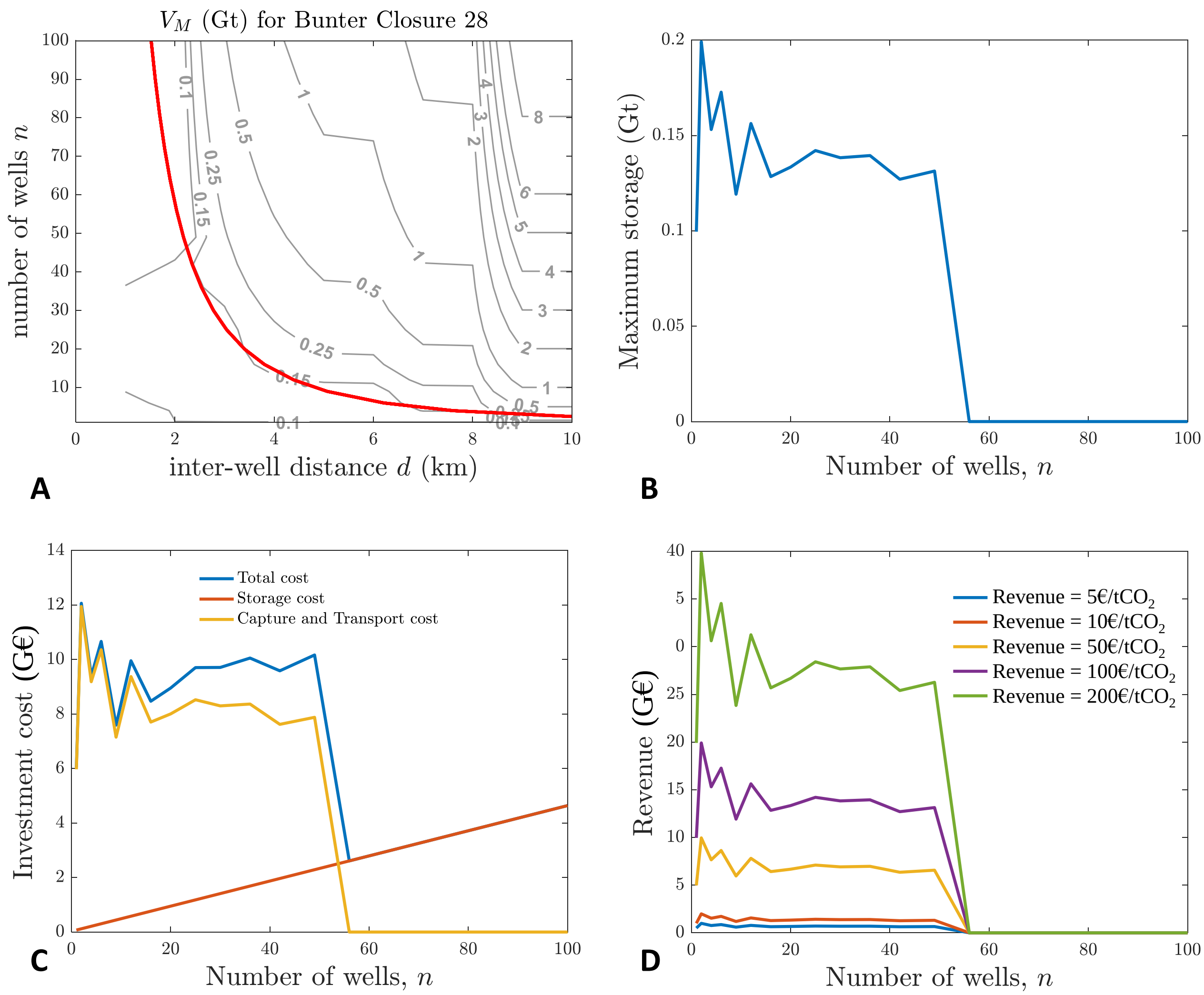

Figure S4: Cost and revenues of 30 years of CO_2 storage at the Bunter Closure 28 site under different scenarios of well number and revenue values. A) Pressure-limited scenarios of sustainable injection mass for different well number and distance; plausible scenarios are on the left of the red line. B) Maximum plausible storage capacity for each scenario of well number (corresponding to the region close to the red line in panel A). C) Investment cost for each scenario of well number represented in panel B. D) Revenues for each scenario of well number represented in panel B and for different values of incentive.

S7 CO2BLOCK details and user guide

CO2BLOCK provides the automatic estimate of the pressure-limited CO_2 storage capacity of an aquifer.

It can be downloaded from the repository https://github.com/co2block/CO2BLOCK. The tool is written in Matlab language and it is composed by six scripts. Users only need to open and modify the script **CO2BLOCK.m**. There is no need to open or modify the other scripts, which is instead not recommended.

Input

It is necessary to provide an input file containing the aquifer parameters data, which must look as presented in the provided example file **example_data.xlsx** (do not change the column order). There is a set of strictly required parameters, whereas others are calculated by means of default values, when not provided (Table S3). Although default values provide reasonable estimations, we recommend the use of precise data which would allow for a more accurate prediction of the storage capacity.

In the **CO2BLOCK.m** script, users have to define directory and name of the input data file. Users also need to set some parameters. They are:

- `correction`: set `on` or `off` to apply correction for superposition (`off` is the most conservative option)
- `dist_min`: minimum inter-well distance [km] (considering operational requirements)
- `dist_max`: maximum inter-well distance [km]. If `auto` is set, the tool automatically calculate the maximum distance according to the reservoir area
- `nr_dist`: number of inter-well distances to explore (high numbers can cause slow calculation)
- `nr_well_max`: maximum number of wells. If `auto` is set, the tool automatically calculate the maximum number of wells according to the reservoir area and the minimum inter-well distance
- `rw`: well radius [m]
- `time_yr`: time of injection [years]
- `maxQ`: maximum sustainable injection rate per well due to technological limitations [Mton/years]

The code work-flow is the following:

1. Acquisition of the parameters by reading the input data
2. Set some parameters with default values if they are not provided in the input data. Details are provided in Table S3.
3. Evaluation of the maximum sustainable pressure
4. Evaluation of the pressure build-up due to a reference injection rate for all the scenarios
5. Estimate of the maximum sustainable injection rate for all the scenarios
6. Inclusion of constraints and rescaling of the maximum injection rates if necessary
7. Evaluation of the plausible scenarios

Output

The tool calculates the storage capacity for each scenario of well number and distance. Output results are the maximum sustainable per-well injection rate and the maximum sustainable injected mass. They are provided both in graphical plots and in .xls tables, as shown in Figure S5.

Table S3: Required and default parameters assumed when not provided.

Required parameters	**Default parameters**	**Default values**
Domain BC (open/closed)	Rock compressibility, c_r	$5{\times}10^{-4}$ MPa^{-1}
Shallowest depth, ζ	Brine compressibility, c_w	$3{\times}10^{-4}$ MPa^{-1}
Mean depth, ζ_m	Brine salinity, χ	180000 ppm
Thickness, H	Shallowest pressure, p_0	10 MPa/km $\times\zeta$
Surface area, A	Mean pressure, $\overline{p_0}$	10 MPa/km $\times\zeta_m$
Permeability, κ	Mean Temperature, $\overline{T_0}$	33°/km $\times\zeta_m + 15°$
Porosity, ϕ	CO_2 density, ρ_c	calculated with respect to $\overline{p_0}$ and $\overline{T_0}$, according to Redlich and Kwong (1949) (with the parameters proposed by Spycher et al. (2003))
	CO_2viscosity, μ_c	calculated with respect to $\overline{p_0}$ and $\overline{T_0}$, according to Altunin and Sakhabetdinov (1972)
	Brine viscosity, μ_w	calculated with respect to $\overline{T_0}$ and χ, according to Batzle and Wang (1992)
	Vertical stress, σ_v	23 MPa/km $\times\zeta_m$
	Stress ratio, k_0	0.7
	Friction coefficient, φ	30°
	Cohesion, C	0 MPa
	Tensile strength, S_0	0 MPa

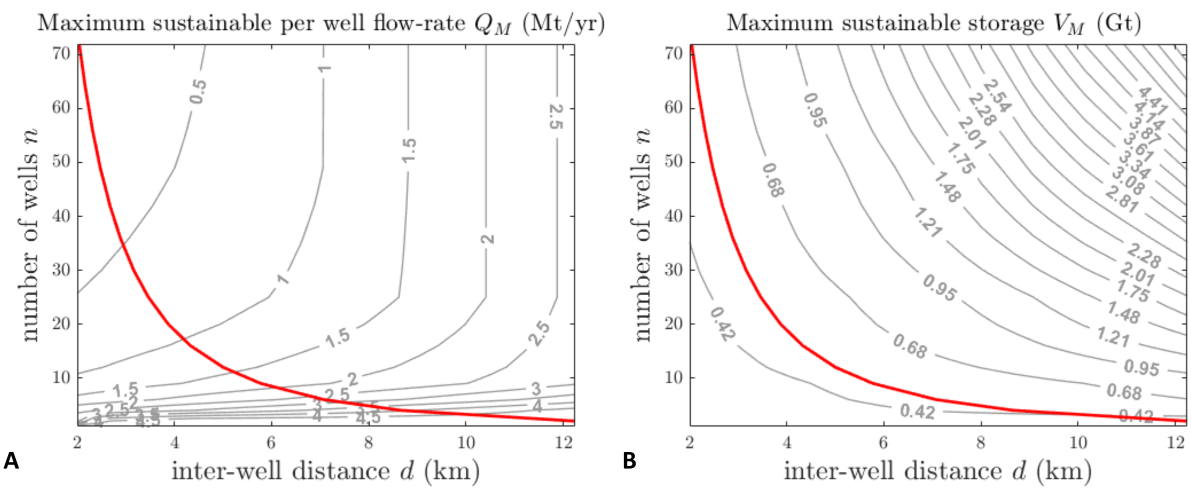

Q_M_max_per_well_inj_rate.xls

number_of_wells	Q_M_for_d_2000_m	Q_M_for_d_2353_m	....
1	4.9995	4.9995	....
2	2.939132945	4.069453454	....
4	2.359490433	2.46777783	....
....	....	....	....

C

V_M_max_per_well_inj_rate.xls

number_of_wells	V_M_for_d_2000_m	V_M_for_d_2353_m	....
1	0.149985	0.149985	....
2	0.176347977	0.244167207	....
4	0.283138852	0.29613334	....
....	....	....	....

D

Figure S5: Examples of CO2BLOCK output plots and tables. Pressure-limited scenarios of sustainable mass injection rate (Mt/yr) (A and C) and of total mass for the injection period (Gt) (B and D) for different number of wells and inter-well distance. In A and B, plausible scenarios are on the left of the red line. In C and D, rows correspond to different scenarios of well number, while columns correspond to different scenarios of inter-well distance.

References

Altunin, V. and Sakhabetdinov, M. (1972). Viscosity of liquid and gaseous carbon dioxide at temperatures 220-1300 K and pressure up to 1200 bar. *Teploenergetika*, 8:85–89.

Batzle, M. and Wang, Z. (1992). Seismic properties of pore fluids. *Geophysics*, 57(11):1396–1408.

Carneiro, J., Martinez, R., Suaréz, I., Zarhloule, Y., and Rimi, A. (2015). Injection rates and cost estimates for CO2 storage in the west mediterranean region. *Environmental earth sciences*, 73(6):2951–2962.

De Simone, S., Jackson, S. J., and Krevor, S. (2019). The error in using superposition to estimate pressure during multi-site subsurface CO2 storage. *Geophysical Research Letters*, 46(12):6525–6533.

Energy Technologies Institute LLP, E. (2018). CO2stored database. http://www.co2stored.co.uk/.

IPCC (2005). IPCC special report on carbon dioxide capture and storage. prepared by working group III of the Intergovernmental Panel on Climate Change. *In: Metz, B., Davidson, O., de Coninck, H.C., Loos, M., Meyer, L.A. (eds.). Cambridge University Press, Cambridge, United Kingdom and New York, NY, USA, 442 pp.*

Mathias, S. A., Gluyas, J. G., Goldthorpe, W. H., and Mackay, E. J. (2015). Impact of maximum allowable cost on CO2 storage capacity in saline formations. *Environmental science & technology*, 49(22):13510–13518.

Nordbotten, J. M., Celia, M. A., and Bachu, S. (2005). Injection and Storage of CO2 in Deep Saline Aquifers: Analytical Solution for CO2 Plume Evolution During Injection. *Transport in Porous Media*, 58(3):339–360.

Redlich, O. and Kwong, J. N. (1949). On the thermodynamics of solutions. V. An equation of state. Fugacities of gaseous solutions. *Chemical reviews*, 44(1):233–244.

Spycher, N., Pruess, K., and Ennis-King, J. (2003). CO2-H2O mixtures in the geological sequestration of CO2. I. assessment and calculation of mutual solubilities from 12 to 100C and up to 600 bar. *Geochimica et cosmochimica acta*, 67(16):3015–3031.

Zimmerman, R. (2018). The Imperial College lectures in petroleum engineering. volume 5: Fluid flow in porous media. *World Scientific Publishing Europe*.